ARTICLE

Theoretical Investigations of the Local Structure Distortion and EPR Parameter for Ni^{2+}-doped Perovskite Fluorides

Xi-min Cao[a], Xiao-yu Kuang[a,b*], Cheng-gang Li[a], Rui-peng Chai[a]

a. Institute of Atomic and Molecular Physics, Sichuan University, Chengdu 610065, China
b. International Centre for Materials Physics, Chinese Academy of Sciences, Shenyang 110016, China

(Dated: Received on November 25, 2010; Accepted on February 14, 2011)

By analyzing the optical spectra and electron paramagnetic resonance parameter D, the local structure distortion of $(NiF_6)^{4-}$ clusters in AMF_3 (A=K, Rb; M=Zn, Cd, Ca) and K_2ZnF_4 series are studied using the complete energy matrix based on the double spin-orbit coupling parameter model for configuration ions in a tetragonal ligand field. The results indicate that the contribution of ligand to spin-orbit coupling interaction should be considered for our studied systems. Moreover, the relationships between D and the spin-obit coupling coefficients as well as the average parameter and the divergent parameter are discussed.

Key words: Complete energy matrix, Double spin-orbit coupling parameter model, Local structure distortion

I. INTRODUCTION

Because doped materials can display a significant role in the ferroelectric, piezoelectric, photoelectric, and ferromagnetic properties which are absent in pure compounds, impurities in solid materials have been a subject of wide interest in recent years [1−4]. Among these impurities, much attention has been paid to the divalent Ni^{2+} since the materials doped with Ni^{2+} always exhibit broad absorption bands in the visible and infrared spectral range [5, 6]. For example, the perovskite fluorides AMF_3 and perovskite-type fluorides K_2ZnF_4 doped with Ni^{2+} ions have attracted much attention because of their particular structures, phase transitions, luminescent and ferromagnetic properties and so on [7−9]. In order to gain more insight into the optical and magnetic properties of the Ni^{2+}-doped perovskite systems, many experimental works have been performed. For instance, the electron paramagnetic resonance (EPR) spectra for the Ni^{2+}-doped AMF_3 and K_2ZnF_4 systems have been reported [10−14]. These experimental results have provided important information for studying the relationships between the electronic and molecular structure of the doped systems. From the theoretical point of view, to explain these experimental EPR spectra and determine the local structure distortion for these systems, two theoretical methods have been proposed, namely, the high-order perturbation and the complete energy matrix. It is noted that the method of complete energy matrix is established in the complete d^n configuration space and all the interactions may be taken into account simultaneously, whereas the high-order perturbation method only considers the partial states. Hence, the approach of complete energy matrix has been widely applied in the studies of EPR parameters D and the local structure of the Ni^{2+} doped systems [15−17].

In the framework of complete energy matrix, as a rule, there are two kinds of models to treat the spin-orbit (s.o.) coupling interaction. One is the single s.o. coupling parameter model, in which only the contribution due to the s.o. coupling of the central ion is considered. This model has been widely used in the past several years [15−17]. The other one is the double s.o. coupling parameter model, which not only includes the contribution arising from the s.o. coupling of central ion, but also considers the effect of surrounding ligand. Evidently the latter model is superior to the former in studying EPR parameters. It is well known that the contribution from the ligand should not be neglected in the exact calculation. In fact, many researches have proved that the influence of ligand ions cannot be ignored with respect to the s.o. coupling mechanism [18, 19]. Thus, the method of complete energy matrix based on the double s.o. coupling parameter model is generally regarded as a more effective tool to study the EPR and local structure distortion of the compounds, and the method of complete energy matrix based on the double s.o. coupling parameter model is used less by researchers at home and abroad.

In the present work, by using the complete energy matrix method and based on the double s.o. coupling parameter model, the D and the local structure distortion parameter ΔR for Ni^{2+} ions doped in AMF_3 and K_2ZnF_4 systems are studied, and the relationships be-

*Author to whom correspondence should be addressed. E-mail: scu_kxy@163.com, Tel./FAX: +86-28-85405515

tween the D and s.o. coupling coefficients (ζ, ζ') as well as the average parameter ζ_1 (ζ_1=(ζ+ζ')/2) and the divergent parameter ζ_2 (ζ_2=(ζ−ζ')/2) are discussed. In addition, the dependence of the D on ΔR is studied together.

II. THEORETICAL ANALYSIS

A. Double s.o. coupling parameter model

Just as remarked by Sugano *et al.* [20], two s.o. coupling coefficients ζ and ζ' should be simultaneously introduced to describe the difference in overlap between $|t_{2g}\rangle$ and $|e_g\rangle$ symmetry from the d orbitals of the central ions and to consider the contribution from the p orbitals of the ligands, which are defined as [20]:

$$\langle t_{2g}|\, v(1T)\, |t_{2g}\rangle = 3i\zeta \tag{1}$$

$$\langle t_{2g}|\, v(1T)\, |e_g\rangle = -3\sqrt{2}i\zeta' \tag{2}$$

where ζ and ζ' may be expressed as [20−22]:

$$\zeta = N_t\left(\zeta_d^0 + \frac{1}{2}\lambda_t^2\zeta_p^0\right) \tag{3}$$

$$\zeta' = \sqrt{N_t N_e}\left(\zeta_d^0 - \frac{1}{2}\lambda_t\lambda_e\zeta_p^0\right) \tag{4}$$

ζ_d^0 and ζ_p^0 represent the s.o. coupling coefficients of the central ion and the ligand ion, respectively. The molecular-orbital wave function can be written as [23]:

$$|\gamma\rangle = \sqrt{N_\gamma}\left(|d_\gamma^0\rangle - \lambda_\gamma|p_\gamma\rangle\right) \tag{5}$$

$|d_\gamma^0\rangle$ is the basic state of the d orbit for central metal ion; $|p_\gamma\rangle$ is the basic state of the p orbit for ligand ion. The subscripts γ=t_{2g} or e_g are the irreducible representations of the O_h group. The normalization factor N_γ and orbital mixing coefficient λ_γ can be obtained from the approximation relation [23]:

$$f_\gamma = N_\gamma^2[1 - 2\lambda_\gamma S_{dp}(\gamma) + \lambda_\gamma^2 S_{dp}^2(\gamma)] \tag{6}$$

and the normalization correlation [23]:

$$N_\gamma[1 - 2\lambda_\gamma S_{dp}(\gamma) + \lambda_\gamma^2] = 1 \tag{7}$$

$S_{dp}(\gamma)$ is the group overlap integrals. The covalency factor f_γ are often determined from the ratio of the Racah parameters for the $3d^8$ ion in a crystal to those in free state, *i.e.*,

$$f_\gamma \approx \frac{1}{2}\left(\frac{B}{B_0} + \frac{C}{C_0}\right) \tag{8}$$

B and C are the Racah parameters of the transition metal ion in the studied crystal and B_0, C_0, ζ_d^0 are the free ion parameters. The values of N_γ, λ_γ, ζ, and ζ' may be obtained from Eqs. (3), (4), (6), and (7).

B. Complete energy matrix for d^8 configuration ions

The perturbation Hamiltonian for a d^8 configuration ion Ni^{2+} in a tetragonal ligand field can be expressed as [24]:

$$\begin{aligned}\hat{H} &= \hat{H}_{\rm ee} + \hat{H}_{\rm SO} + \hat{H}_{\rm LF} \\ &= \sum_{i<j}\frac{e^2}{r_{i,j}} + \sum_i \zeta_d^0(r_i)\hat{l}_i\cdot\hat{s}_i + \\ &\quad \sum_j \zeta_p^0(r_j)\hat{l}_j\cdot\hat{s}_j + \sum_i V_i\end{aligned} \tag{9}$$

where $\hat{H}_{\rm ee}$, $\hat{H}_{\rm SO}$, and $\hat{H}_{\rm LF}$ denote the electron-electron repulsion interaction, the s.o. coupling interaction, and the ligand-field interaction, respectively. The potential function V_i can be written as:

$$\begin{aligned}V_i = \gamma_{00}Z_{00} + \gamma_{20}r_i^2 Z_{20}(\theta_i,\varphi_i) + \gamma_{40}r_i^4 Z_{40}(\theta_i,\varphi_i) + \\ \gamma_{44}^c r_i^4 Z_{44}^c(\theta_i,\varphi_i) + \gamma_{44}^s r_i^4 Z_{44}^s(\theta_i,\varphi_i)\end{aligned} \tag{10}$$

where r_i, θ_i, and φ_i are spherical coordinates of the ith electron. Z_{lm} and Z_{lm}^c are defined as:

$$Z_{l0} = Y_{l0} \tag{11}$$

$$Z_{lm}^c = \frac{1}{\sqrt{2}}[Y_{l,-m} + (-1)^m Y_{l,m}] \tag{12}$$

$$Z_{lm}^s = \frac{i}{\sqrt{2}}[Y_{l,-m} - (-1)^m Y_{l,m}] \tag{13}$$

$Y_{l,m}$ is the spherical harmonics. γ_{l0} and γ_{lm}^c are associated with the local lattice structure of the $3d^8$ configuration ion by the relations

$$\gamma_{l0} = -\frac{4\pi}{2l+1}\sum_{\tau=1}^{n}\frac{eq_\tau}{R_\tau^{l+1}}Z_{l0}(\theta_\tau,\varphi_\tau) \tag{14}$$

$$\gamma_{lm}^c = -\frac{4\pi}{2l+1}\sum_{\tau=1}^{n}\frac{eq_\tau}{R_\tau^{l+1}}Z_{lm}^c(\theta_\tau,\varphi_\tau) \tag{15}$$

$$\gamma_{lm}^s = -\frac{4\pi}{2l+1}\sum_{\tau=1}^{n}\frac{eq_\tau}{R_\tau^{l+1}}Z_{lm}^s(\theta_\tau,\varphi_\tau) \tag{16}$$

where q_τ is the effective charge of the τth ligand ion, θ_τ and φ_τ are its angle coordinates, R_τ is the impurity-ligand distance. The ligand-field interaction in the tetragonal field is the function of four parameters B_{20}, B_{40}, B_{44}^c, and B_{44}^s. By choosing the appropriate coordinate system, the ligand-field parameter B_{44}^s will vanish and B_{20}, B_{40}, B_{44}^c can be derived as:

$$B_{20} = 2A_2\left(\frac{1}{{R_1}^3} - \frac{1}{{R_2}^3}\right) \tag{17}$$

$$B_{40} = \frac{A_4}{2}\left(\frac{4}{{R_1}^5} + \frac{3}{{R_2}^5}\right) \tag{18}$$

$$B_{44}^c = \sqrt{\frac{35}{8}}\frac{A_4}{{R_2}^5} \tag{19}$$

DOI:10.1088/1674-0068/24/02/167-172

TABLE I The local structure distortion parameter (in Å), group overlap integrals, B and C, f_r, N_r, N_e, and λ_t, λ_e, s.o. coupling coefficients ζ and ζ', average ζ_1 and divergent ζ_2 parameters (cm^{-1}) for Ni^{2+} in crystals.

	$\bar{R}$	S_{dpt}	S_{dpe}	B^a	C^a	f_r	N_t	N_e	λ_t	λ_e	ζ	ζ'	ζ_1	ζ_2
K_2ZnF_3(4.2 K)	2.0207	0.0244	0.0065	972	3588	0.8047	0.899	0.9048	0.3417	0.3498	583.775	562.191	572.983	10.7920
K_2ZnF_3(78 K)	2.0201	0.0245	0.0065	972	3588	0.8047	0.899	0.9048	0.3417	0.3498	583.779	562.197	572.988	10.7910
K_2ZnF_3(290 K)	2.0168	0.0248	0.0066	972	3588	0.8047	0.899	0.9049	0.3418	0.3500	583.800	562.229	573.015	10.7855
$KZnF_4$	2.0607	0.0212	0.0055	972	3588	0.8047	0.899	0.9037	0.3413	0.3483	583.541	561.831	572.686	10.8550
$RbCaF_3$	2.0883	0.0192	0.0049	950	4000	0.8417	0.9188	0.923	0.3022	0.3088	594.059	576.690	585.375	8.6845
$RbCdF_3$	2.0848	0.0195	0.005	950	4000	0.8417	0.9189	0.923	0.3022	0.3089	594.074	576.714	585.394	8.6800

[a] Refs.[30, 31].

where R_1 and R_2 stand for the bond lengths in the vertical plane and the horizontal plane in tetragonal D_{4h} symmetry, respectively. In the previous works, the values of A_4 and A_2 have been determined from the optical spectra and local structure of pure NiF_2 [25], *i.e.*, A_4≈17.3385 a.u. and A_2≈2.4452 a.u., and these will be employed in the following calculation.

C. EPR parameters of d^8 configuration

EPR spectra of a d^8 configuration Ni^{2+} in a tetragonal ligand-field can be analyzed by the spin Hamiltonian [26]:

$$\hat{H}_S = \mu_B g_{//} H_z S_z + \mu_B g_\perp (H_x S_x + H_y S_y) + D\left[{S_z}^2 - \frac{1}{3}S(S+1)\right] \quad (20)$$

In the absence of the external magnetic field, the ground state $^3A_2$ is split into two spin doublets $|\pm 1\rangle$ and $|0\rangle$. The corresponding ground-state zero-field splitting ΔE can be expressed as:

$$\Delta E = E(\pm 1) - E(0) = D \quad (21)$$

III. CALCULATIONS AND DISCUSSION

A. Calculation of the local structure for tetragonal Ni^{2+} centers

According to the EPR spectra of the Ni^{2+}-doped AMF_3 and K_2ZnF_4 series, we can study the local geometric structure by diagonalizing the complete energy matrix. When the Ni^{2+} is doped into the host crystal, it will substitute for the divalent cation M^{2+}. The local structure belongs to D_{4h} symmetry and displays a tetragonal distortion along fourfold axis, and it can be described by use of R_1 and R_2 as shown in Fig.1. R_1 is the distance between Ni^{2+} and the two axial F^- ligands in the vertical plane, R_2 is the distance between Ni^{2+} and the four equatorial F^- ligands in the horizontal plane, and the ΔR and $\bar{R}$ can be expressed as:

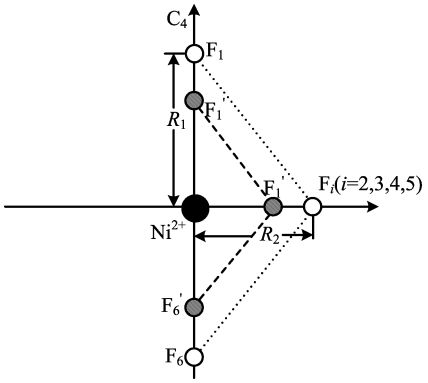

FIG. 1 The local structure distortion for $(NiF_6)^{4-}$ cluster in perovskite fluorides. R_1 is the distance between Ni^{2+} and the two axial F_i^- (i=1, 6) ligands in the vertical plane, R_2 is the distance between Ni^{2+} and the four equatorial F_i^- (i=2, 3, 4, 5) ligands in the horizontal plane.

$$\bar{R} = \frac{1}{3}R_1 + \frac{2}{3}R_2, \quad \Delta R = R_1 - R_2 \quad (22)$$

$\bar{R}$ may be obtained through simulating the optical spectra of the $(NiF_6)^{4-}$ cluster in different perovskite hosts by diagonalizing the complete energy matrix. For the free Ni^{2+}, B_0≈1208 cm^{-1}, C_0≈4495 cm^{-1}, and ζ_d^0≈636.5 cm^{-1}, ζ_p^0≈220 cm^{-1} for F^- [23, 27]. The group overlap integrals $S_{dp}(\gamma)$, two s.o. coupling coefficients ζ and ζ' may be calculated from the Slater-type SCF function [28, 29]. The corresponding values are listed in Table I. Then, by diagonalizing the complete energy matrix, the optical spectra and D for the Ni^{2+} ions in different crystals are simulated as functions of ΔR. The calculated results are listed in Table II and III. It is noticeable in Table III that the calculated Stark energy levels are in good agreement with the experimental values. D can be satisfactorily explained by the obtained ΔR as shown in Table II. For the Ni^{2+}-doped $RbCdF_3$ and $RbCaF_3$ systems, the local lattice structures around the octahedral Ni^{2+} centers display an

DOI:10.1088/1674-0068/24/02/167-172

TABLE II The local distortion parameter ΔR and EPR parameter D for K_2ZnF_4:Ni^{2+}, $KZnF_3$:Ni^{2+}, $RbCaF_3$:Ni^{2+}, and $RbCdF_3$:Ni^{2+} systems which are calculated from different models.

Compound	ΔR/Å		$r_{\Delta R}$	D/cm^{-1}		
	Cal.[a]	Cal.[b]		Cal.[a]	Cal.[b]	Expt. [10−14]
K_2ZnF_3:Ni^{2+}(4.2 K)	−0.0414	−0.0314	24%	−1.2399	−1.2399	−1.24(1)
K_2ZnF_3:Ni^{2+}(78 K)	−0.0433(2)	−0.0329	24%	−1.31	−1.3104	−1.31
K_2ZnF_3:Ni^{2+}(290 K)	−0.0532	−0.0408	23%	−1.6701	−1.6703	−1.67
$KZnF_3$:Ni^{2+}	−0.0144(4)	−0.0065	55%	−0.2501	−0.25	−0.2497
$RbCaF_3$:Ni^{2+}	0.0136(2)	0.0193	30%	0.8441	0.8438	0.844(2)
$RbCdF_3$:Ni^{2+}	0.0032(4)	0.0093	66%	0.4078	0.4075	0.408(1)

[a] Calculated from the complete energy matrix based on the double s.o. coupling parameter model.
[b] Calculated from the complete energy matrix based on the single s.o. coupling parameter model [15, 16, 28].

TABLE III Comparison of optical spectra between the theoretical and experimental values for Ni^{2+} ions in K_2ZnF_4 (4.2 K), $KZnF_3$, and $RbCaF_3$ crystals, respectively.

	K_2ZnF_4(4.2 K)		$KZnF_3$		$RbCaF_3$	
	Exp. [32]	Cal.	Exp. [33]	Cal.	Exp. [34]	Cal.
$^3A_2(F)$	0	0	0	0	0	0
$^3T_2(F)$	7550	7550	7000	7000		6590
		7942		7123	6700	6699
$^3T_1(F)$	12965	13091		11999		11243
		13347	12800	12074	11400	11307
$^1E(D)$	15313	14237		14232		14867
		14289	14900	14234	15000	14876
$^1T_2(F)$	21050	21373		20733	20000	20961
		21737	21100	20851		21066
$^1A_1(G)$	24360	23349		23006		23443
$^3T_1(P)$		24760	24000	23765	22500	22770
		25130		23892		22886
$^1T_1(G)$		26394		25832		25861
		27248		26111		21662
$^1E(G)$	30675	32075		30756		30486
		32382		30857		30575

elongated distortion along the C_4 axis; and for the Ni^{2+}-doped $KZnF_3$ and K_2ZnF_4 systems, the local structures display a compressed distortion along the C_4-axis.

In order to study the difference between the double s.o. coupling coefficient model and the single s.o. coupling coefficient model, we simulate D at the same ΔR using the two models, the calculated results are presented in Table II. By comparison, we found that the local structure distortion parameters obtained from the double s.o. coupling parameter model differ from that obtained from the single s.o. coupling parameter model. Although the discrepancy of ΔR based on the two models varies with the different hosts, the difference for all the studied systems is appreciable as shown in Table II. For example, for the K_2ZnF_4 host the relative error

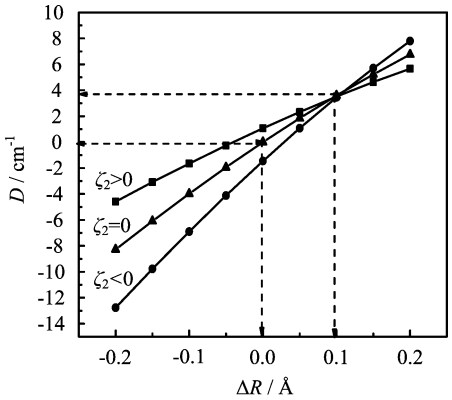

FIG. 2 The influence of ΔR on D with different ζ_2 for K_2ZnF_4:Ni^{2+} system.

$r_{\Delta R}$,

$$r_{\Delta R} = \frac{|\Delta R_a - \Delta R_b|}{|\Delta R_{\max}|} \times 100\% \tag{23}$$

which accounts for about 23%, and for the $RbCdF_3$ host the relative error is somewhat large and accounts for about 66%. The reason may be ascribed to the contribution of the s.o. coupling interaction from the ligands. Since the double s.o coupling parameter model is superior to the single s.o. coupling parameter model, the local structure distortion parameters ($\bar{R}$, ΔR) based on the double s.o. coupling parameter model can be regarded as more accurate and reliable. Simultaneously, the difference of ΔR also indicates that the contribution of the s.o. coupling interaction of F^- ligands on the local structure distortion of the central ions in the perovskite fluorides is not negligible.

Figure 2 shows the relationship between D and ΔR for the K_2ZnF_4:Ni^{2+} system with ζ_2=0, ζ_2>0, and ζ_2<0, based on both of the double and single s.o. coupling parameter models. It indicates that there is an approximate linear relation between ΔR and D, and the values of D will increase with the increase of ΔR. Simultaneously, it is found that for ζ_2=0 (namely, the

DOI:10.1088/1674-0068/24/02/167-172

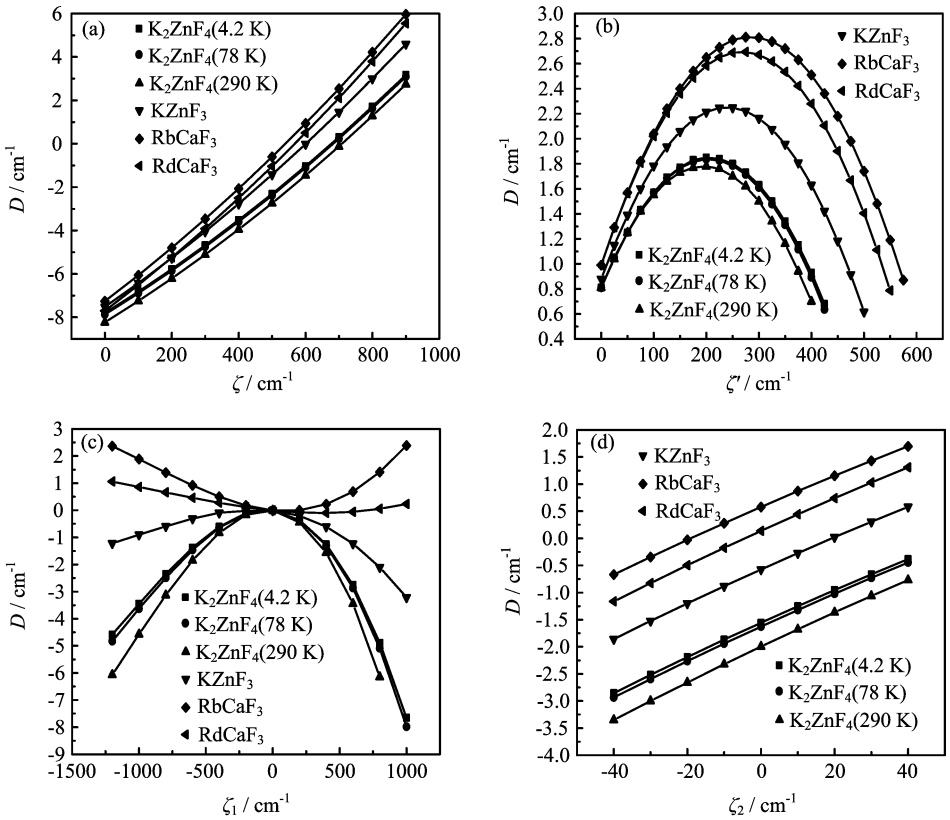

FIG. 3 Dependence of D on ζ (a) and ζ' (b) for Ni^{2+}-doped AMF_3 (A=K, Rb; M=Zn, Cd, Ca) and K_2ZnF_4, respectively. Variation of ζ_1 (c) and ζ_2 (d) versus D for the Ni^{2+}-doped AMF_3 (A=K, Rb; M=Zn, Cd, Ca) and K_2ZnF_4 series.

case of the single s.o. coupling model), when ΔR=0, then D=0; when $\Delta R \neq 0$, the sign of D is the same as the sign of ΔR. However, for $\zeta_2>0$ and $\zeta_2<0$, the point of ΔR=0 corresponds to $D>0$ and $D<0$, respectively. Moreover, all the three curves converge when $\Delta R \approx 0.1$ Å. The calculated results of local structure distortion parameters in Table II may be well explained using the relative curves of Fig.2.

B. The effects of ζ or ζ', ζ_1, and ζ_2 on D

As mentioned above, the s.o. coupling coefficients ζ and ζ' are introduced by Sugano *et al.* [20]. For our studied systems, the relationships of D *vs.* ζ and D *vs.* ζ' are shown in Fig.3 (a) and (b). It should be remarked that D is directly linear relation to ζ and proportional to the square of ζ' based on the method of high order perturbation. However, our calculated results show that the curve of D *vs.* ζ is not strictly linear relation (see Fig.3(a)), as well as D *vs.* ζ' is not strictly quadratic relation (see Fig.3(b)). This difference may be due to the fact that the complete energy matrix method involves all microstates of the d^8 configuration, whereas only the part microstates of the d^8 configuration are considered in the high order perturbation method.

The relationships of D *vs.* ζ_1 and D *vs.* ζ_2 have been plotted in Fig.3 (c) and (d) with the different hosts. From Fig.3(c), it can be seen that the curve of D *vs.* ζ_1 is approximately quadratic. Meanwhile, all the relative curves pass the same point (0, 0), because ζ_1=0 is related to D=0 with the cubic symmetric structure. Moreover, it can be seen that from Fig.3(c), when $D>0$, and the direction of the $D(\zeta_1)$ is upward, when $D<0$, and the direction of $D(\zeta_1)$ is downward. These trends may be ascribed to the fact that there is a corresponding relationship between the direction of $D(\zeta_1)$ and the local structure distortion for the $(NiF_6)^{4-}$ clusters. At last, the relation of D *vs.* ζ_2 has been plotted in Fig.3(d). It is noticeable that there exists an approximately linear relation between the D and ζ_2 in the range of ζ_2 from -40 cm^{-1} to 40 cm^{-1}, and the value of D will increase with the increase of ζ_2 for all curves.

IV. CONCLUSION

Using the complete energy matrix method and taking into account the contributions from the s.o. coupling of the central ions as well as that of the ligand ions, the optical spectra, the EPR parameter D and the local structure distortion for the AMF_3 (A=K, Rb; M=Zn, Cd, Ca) and K_2ZnF_4 doped with Ni^{2+} ions have been studied. The results indicate that the contribution of

DOI:10.1088/1674-0068/24/02/167-172

the s.o. coupling interaction for F^- ligands on the local structure distortion of the central ions in the perovskite fluorides is not negligible. Moreover, the relationship between D and ΔR and the dependences of D on the s.o coupling coefficients ζ (ζ', ζ_1, and ζ_2) have been demonstrated.

[1] K. Ragavendran, A. Nakkiran, P. Kalyani, A. Veluchamy, and R. Jagannathan, Chem. Phys. Lett. **110**, 456 (2008).
[2] T. Wang, A. A. Wu, L. G. Gao, and H. Q. Wang, Chin. J. Chem. Phys. **22**, 51 (2009).
[3] J. Pisarska, W. A. Pisarski, G. Dominiak, and W. R. Romanowski, J. Mol. Struct. **201**, 792 (2006).
[4] Z. Y. Yang and Q. Wei, Chin. J. Chem. Phys. **17**, 401 (2004).
[5] S. C. Zhang, H. P. Xia, J. H. Wang, and Y. P. Zhang, J. Alloys Compd. **463**, 446 (2008).
[6] B. T. Wu, N. Jiang, S. F. Zhou, D. P. Chen, C. S. Zhu, and J. R. Qiu, Opt. Mater. **30**, 1900 (2008).
[7] R. N. Hua, Z. H. Jia, D. M. Xie, and C. S. Shi, Mater. Res. Bull. **37**, 1189 (2002).
[8] W. C. Zheng, P. Ren, and S. Y. Wu, Phys. B **291**, 123 (2000).
[9] A. E. Lavata and E. J. Baran, J. Alloys Compd. **419**, 334 (2006).
[10] Y. Yamaguchi, Solid State Commun. **11**, 1611 (1972).
[11] S. N. Lukin, Sov. Phys. Sol. Stat. **11**, 711 (1972).
[12] Y. Tomono, T. Kato, and Y. Tanokura, J. Phys. Soc. Jpn. **53**, 773 (1984).
[13] P. J. Alonso, R. Alcala, and J. M. Spaeth, Phys. Rev. B **41**, 10902 (1990).
[14] B. Villacampa, R. Alcalt, P. J. Alonso, and J. M. Spaeth, J. Phys.: Condens. Matter **5**, 747 (1993).
[15] S. J. Wang, X. Y. Kuang, and C. Lu, Spectrochim. Acta A **71**, 1317 (2008).
[16] H. F. Li, X. Y. Kuang, and H. Q. Wang, Chem. Phys. Lett. **462**, 133 (2008).
[17] H. Q. Wang, X. Y. Kuang, and H. F. Li, Chem. Phys. Lett. **460**, 365 (2008).
[18] C. G. Li, X. Y. Kuang, R. P. Chai, and Y. R. Zhao, Chem. Phys. Lett. **498**, 353 (2010).
[19] Z. X. Yan, X. Y. Kuang, M. L. Duan, C. G. Li, and R. P. Chai, Mol. Phys. **108**, 1899 (2010).
[20] S. Sugano, Y. Tanabe, and H. Kamimura, *Multiplets of Transition Metal Ions in Crystals*, New York: Academic, (1970).
[21] D. Curie, C. Barthon, and B. Canny, J. Chem. Phys. **61**, 3048 (1974).
[22] M. G. Zhao, J. A. Xu, G. R. Bai, and H. S. Xie, Phys. Rev. **27**, 1516 (1983).
[23] M. L. Du and C. Rudowicz, Phys. Rev. B **46**, 8974 (1992).
[24] (a) X. Y. Kuang, Phys. Rev. B **36**, 712 (1987);
(b) M. L. Du and C. Rudowicz, **36**, 797 (1987).
[25] Y. R. Zhao, X. Y. Kuang, C. Lu, M. L. Duan, and B. B. Zheng, Mol. Phys. **107**, 133 (2009).
[26] A. Abragam and B. Bleaney, *Electron Paramagnetic Resonance of Transition Ions*, Oxford: Oxford University Press, (1970).
[27] J. S. Griffith, *The Theory of Transition-Metal Ions*, London: Cambridge University Press, (1964).
[28] E. Clementi and D. L. Raimondi, J. Chem. Phys **38**, 2686 (1963).
[29] E. Clementi, D. L. Raimondi, and W. P. Reinhardt, J. Chem. Phys. **47**, 1300 (1967)
[30] M. G. Zhao, M. L. Du, and G. Y. Sen, J. Phys. C **20**, 5557 (1987).
[31] R. Alcala, J. C. Gonzalez, B. Villacampa, and P. J. Alonso, J. Lumin. **48-49**, 569 (1991).
[32] J. S. Tiwari, A. Mehra, and K. G. Srivastava, Jpn. J. Appl. Phys. **7**, 506 (1968).
[33] M. V. Iverson and W. A. Sibley, J. Lumin. **20**, 311 (1979).
[34] B. Villacampa, R. Alcala, P. J. Alonso, and J. M. Spaeth, J. Phys.: Condens. Matter. **747**, 5 (1993).

DOI:10.1088/1674-0068/24/02/167-172